DNA damage and growth hormone hypersecretion in pituitary somatotroph adenomas

Anat Ben-Shlomo, Nan Deng, Evelyn Ding, Masaaki Yamamoto, Adam Mamelak,

Vera Chesnokova, Artak Labadzhyan, Shlomo Melmed

Supplemental Information

Table S1 – Table S3

Figure S1 – Figure S12

Table S1. Genes with sgSCNA processed by KEGG pathway analysis.

AATK	B3GALT2	CCDC181	DIEXF	FCRL4	GRIN3A	KCTD5	MIA3	NWD2	PRR12	SH3TC1	TANC2	UHRF1BP1L	ZNF264
ABCA13	B3GALT6	CCDC190	DIP2B	FEM1B	GRIN3B	KDM5B	MICAL3	ORM1	PRR14L	SHB	TARBP1	UIMC1	ZNF267
ABCB1	BARD1	CCDC66	DLGAP5	FER1L6	GRK7	KIAA0232	MIOS	OTUD7A	PRR16	SHH	TAS2R3	UPK3B	ZNF283
ACE	BAZ2B	CCR2	DLX6	FEV	HADHA	KIAA0430	MKI67	P2RY14	PRR18	SHISA7	TAS2R39	UPP2	ZNF287
ACIN1	BBS10	CCSER1	DMRTA1	FGD6	HAS2	KIAA0753	MKKS	PAIP1	PRRT4	SIK1	TAS2R60	URAD	ZNF292
ACP6	BBS7	CCT7	DMRTA2	FGL2	HCFC1	KIAA1107	MME	PAPD5	PRSS1	SIPA1L2	TBR1	USF3	ZNF304
ACSBG2	BBX	CD163	DMXL2	FIGNL1	HCFC2	KIAA1109	MON2	PARP14	PRSS16	SIPA1L3	TBX1	USP34	ZNF318
ACSS1	BCAS1	CD163L1	DOCK3	FILIP1	HCN4	KIAA1210	MS4A1	PARP15	PTGER1	SIRPB1	TBX2	USP40	ZNF326
ADAMTS12	BCL11A	CD180	DRD4	FLG2	HEATR6	KIAA1551	MTERF1	PARP2	PTK2	SIX4	TCHHL1	USP53	ZNF334
ADAMTSL2	BCLAF1	CD1C	DSE	FLT4	HECTD1	KIF2B	MUM1L1	PARP8	PTPRJ	SKIDA1	TDP1	USPL1	ZNF343
ADARB2	BCR	CDH19	DST	FMN2	HECTD3	KIF3A	MUT	PARP9	PTPRZ1	SLC12A6	TDRD6	UTS2R	ZNF347
ADCY10	BDP1	CDH22	DTL	FNIP1	HELB	KIR3DL2	MXRA8	PARVA	PTRF	SLC15A4	TET2	VCAN	ZNF354B
ADGRL1	BEGAIN	CDHR2	DUSP5	FOXC1	HELZ	KLHL35	MYCN	PAXBP1	PUS3	SLC16A12	TEX15	VEGFA	ZNF354C
ADGRL2	BEND4	CDK13	DYTN	FOXC2	HERC1	KLK9	MYH1	PCDH15	PUS7L	SLC22A25	TGS1	VPS13C	ZNF396
AFDN	BFSP1	CDKN2AIP	EBF3	FOXL2	HES1	KMT2A	MYH2	PCDH18	PYGO1	SLC26A2	THAP9	VWC2L	ZNF416
AFF2	BHLHA9	CEBPA	EDA	FOXQ1	HGFAC	KNL1	MYH4	PCDH9	QSER1	SLC2A12	THBD	WAPL	ZNF440
AGMAT	BHLHB9	CEBPD	EDNRA	FPR3	HIC1	KRT26	MYH8	PCDHA10	R3HCC1L	SLC30A1	THNSL1	WDR33	ZNF451
AGRN	BHLHE41	CEBPZ	EFL1	FRAS1	HIVEP1	KRT33B	MYO16	PCDHA6	RAB3GAP1	SLC30A10	THRB	WDR7	ZNF454
AGTR1	BHMT2	CECR6	EID2	FREM2	HIVEP2	KRT34	MYO9A	PCDHAC1	RAB3IP	SLC35E1	TIGD4	WDR89	ZNF471
AHDC1	BICD1	CEL	EIF4G3	FUCA2	HMCN1	KRT7	N4BP2	PCDHB16	RAG2	SLC39A6	TIGD6	WHSC1L1	ZNF483
AHR	BLOC1S3	CELA3A	ELFN2	FUT4	HMGXB3	KRT77	NANOS1	PCDHB5	RALGAPB	SLC8A2	TLR10	WNK1	ZNF484
AKAP13	BMP2	CENPF	EMX2	FUT9	HMX1	KRTAP10-6	NANP	PCDHGA4	RANBP2	SLC9A5	TLR2	WNK3	ZNF497
AKAP14	BMP2K	CEP152	EN2	FZD3	HS6ST3	LAMA5	NAPRT	PCDHGA6	RAPGEF2	SLCO1B3	TLR5	XIRP2	ZNF510
AKAP3	BOD1L1	CEP170B	ENAM	GAB1	HSPA4L	LCOR	NAT1	PDCD2	RAPH1	SLFN14	TMCC1	XPO1	ZNF514
AKAP6	BRCA1	CEP250	ENDOD1	GABPA	HYAL4	LEMD2	NAV3	PDGFRA	RBAK	SLK	TMEM121	XRN2	ZNF518B
AKAP9	BRCA2	CEP295	ERBB3	GABRA6	ID4	LENG9	NCALD	PDIK1L	RBMXL3	SMC1B	TMEM132D	YOD1	ZNF529
ALDH5A1	BRD8	CEP350	ERBIN	GABRB3	IDUA	LGR4	NCKAP1L	PDZD8	REL	SMCHD1	TMEM133	YY1	ZNF534
ALMS1	BRWD1	CFHR3	ERC2	GAL3ST3	IFFO2	LGSN	NCKAP5L	PDZRN4	REV3L	SMG1	TMEM158	ZAR1	ZNF544
ALS2CR11	BTBD1	CHD2	ERCC4	GALM	IFI16	LHCGR	NCOA1	PEG3	RGAG1	SNED1	TMEM178A	ZBED6	ZNF546
ALYREF	BTBD11	CHML	ERCC6	GALR3	IFIT2	LIG4	NES	PEX1	RLF	SOBP	TMEM64	ZBTB49	ZNF549
AMER2	BTN3A1	CHRNA7	ERCC6L2	GAPVD1	IFNA5	LILRA6	NEURL1	PGP	RLIM	SOCS4	TMEM99	ZCCHC6	ZNF550
AMH	C10orf12	CHST13	ERMAP	GAREM2	IGFL3	LILRB2	NEUROG2	PHF14	RLN2	SOD3	TMPO	ZDBF2	ZNF569
ANGPTL1	C14orf177	CHSY3	ERRFI1	GCC2	IGSF10	LILRB5	NFIA	PHF3	RMI1	SOGA3	TNFAIP3	ZEB2	ZNF573
ANK3	C17orf96	CIC	ERVV-1	GCNT1	IL1RAP	LIPG	NFIB	PHIP	RNASE11	SORBS2	TNFRSF11B	ZFHX4	ZNF583
ANKRD1	C18orf63	CLCNKA	EXD3	GGN	IL6ST	LOR	NIPBL	PHLPP1	RNF139	SOWAHB	TNRC18	ZFP1	ZNF585A
ANKRD11	C1QL1	CLCNKB	EXPH5	GIMAP2	INPP5F	LRBA	NKRF	PIGM	RNF150	SOX1	TOPORS	ZFP28	ZNF587
ANKRD17	C1QTNF4	CLDN17	F11	GIMAP8	INSM1	LRFN1	NKTR	PIK3R1	RNF6	SOX11	TOR4A	ZFP36L2	ZNF596

Table S2. Characteristics of 40 pituitary adenomas included in Western blot and qRT-PCR analysis.

			Gonadotroph & null cell (n=16)	Somatotroph (n=15)	Lactotroph (n=9)
Age, mean ± SD [range]			47.9 ± 17.5 [25-77]	44.8 ± 12.4 [17-64]	45.0 ± 16.9 [23-70]
Sex, n (%)		Females	4 (25.0)	7 (46.6)	3 (33.3)
		Males	12 (75.0)	8 (53.3)	6 (66.7)
IHC	Hormones, n (%)	FSH	14 (80.0)	2 (13.3)	0
		LH	6 (37.5)	1 (6.7)	0
		αGSU	12 (75.0)	7 (46.7)	1 (11)
		ACTH	1 (6.3)	3 (20.0)	1 (11)
		PRL	0	11 (73.3)	9 (100)
		GH	0	15 (100)	0
		TSH	1 (6.3)	4 (26.7)	0
	Ki67, % cells	Mean ± SD	1.4 ± 0.8	1.1 ± 0.8	2.2 ± 1.6
		Median	2	1	2.0
		≥ 3 %	0	2	3
MRI	Largest tumor diameter, mm	Mean ± SD	27.3 ± 11.4	14.5 ± 8.3	21.7 ± 11.3
		Median	26.0	12.5	21
		Range	11-59	2.5-30	6-44
	Adenoma extension, n (%)	Cavernous sinus	11 (68.8)	5 (33.3)	5 (55.6)
		Suprasellar	15 (93.8)	8 (53.3)	3 (33.3)
		Sphenoid sinus	3 (18.8)	4 (26.7)	2 (22.2)
Pre-surgery treatment, n (%)		Dopamine agonist	3 (18.8)	0	9 (100.0)
		Irradiation	0	0	0

IHC, immunohistochemistry

Table S3. Antibodies used in Western blot analysis.

Antibody	Company	Catalogue number	Reactivity*	Clonality
p53	R&D systems	AF1355	H	Polyclonal
$p21^{Wif1/Cip1}$	Cell Signaling	2947	H	Monoclonal
$\gamma H2AX^{Ser139}$	Cell Signaling	9718	H, M	Monoclonal
H2AX	R&D systems	MAB3406	H, M	Monoclonal

*Relevant to this study. H, human; M, mouse

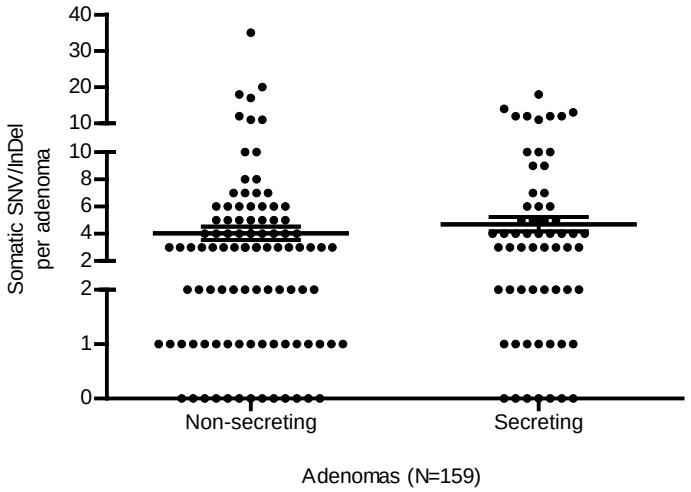

Figure S1. Number of somatic SNV/InDel per adenoma assessed by WES in non-secreting (gonadotroph, null cell, and silent corticotroph; n=98) compared with secreting (corticotroph, lactotroph, and somatotroph; n=61) adenomas.

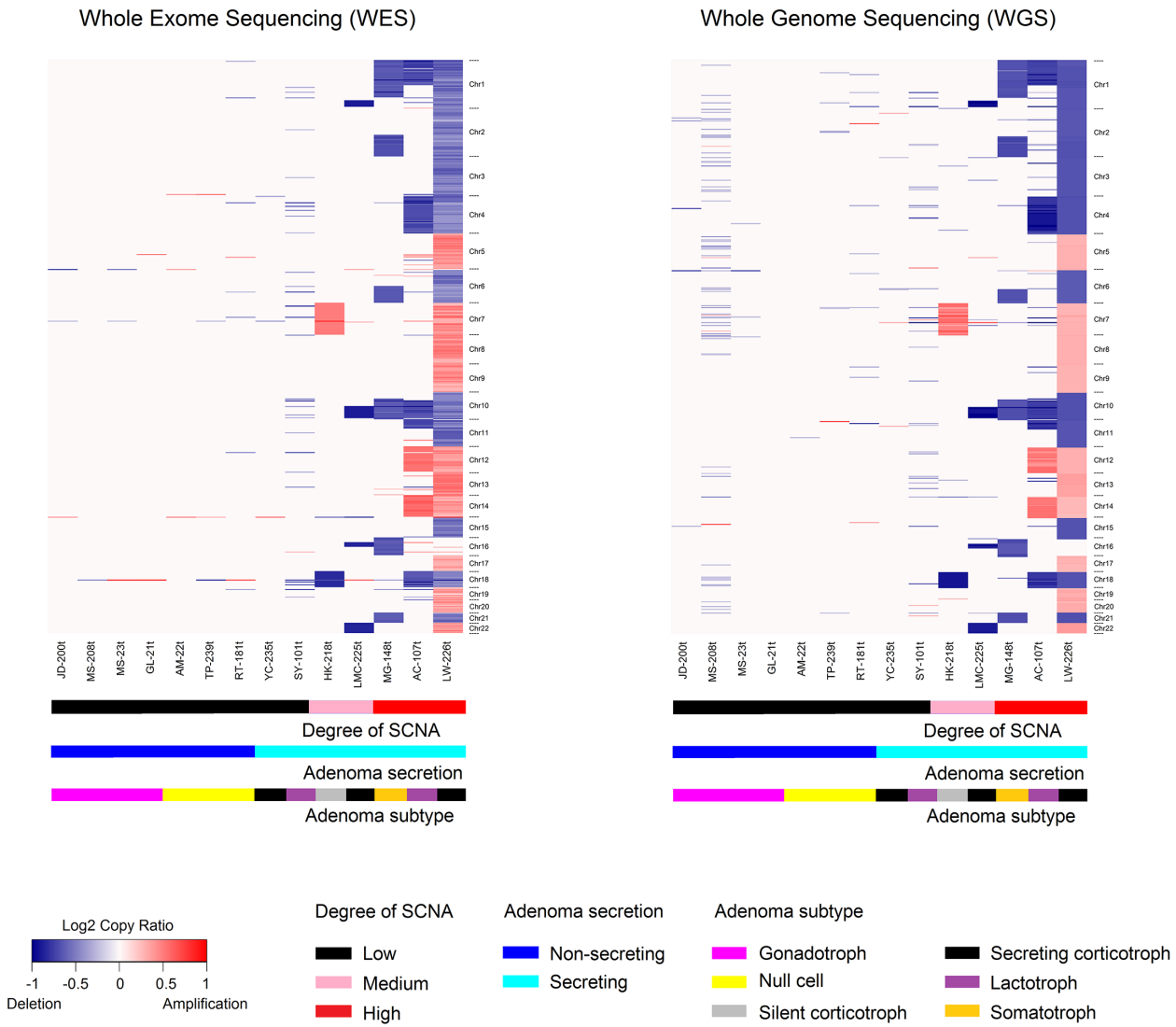

Figure S2. Heatmap of SCNA in 14 pituitary adenomas analyzed by WES and WGS depicting SCNA copy ratio, adenoma functional secretory status, and subtype.

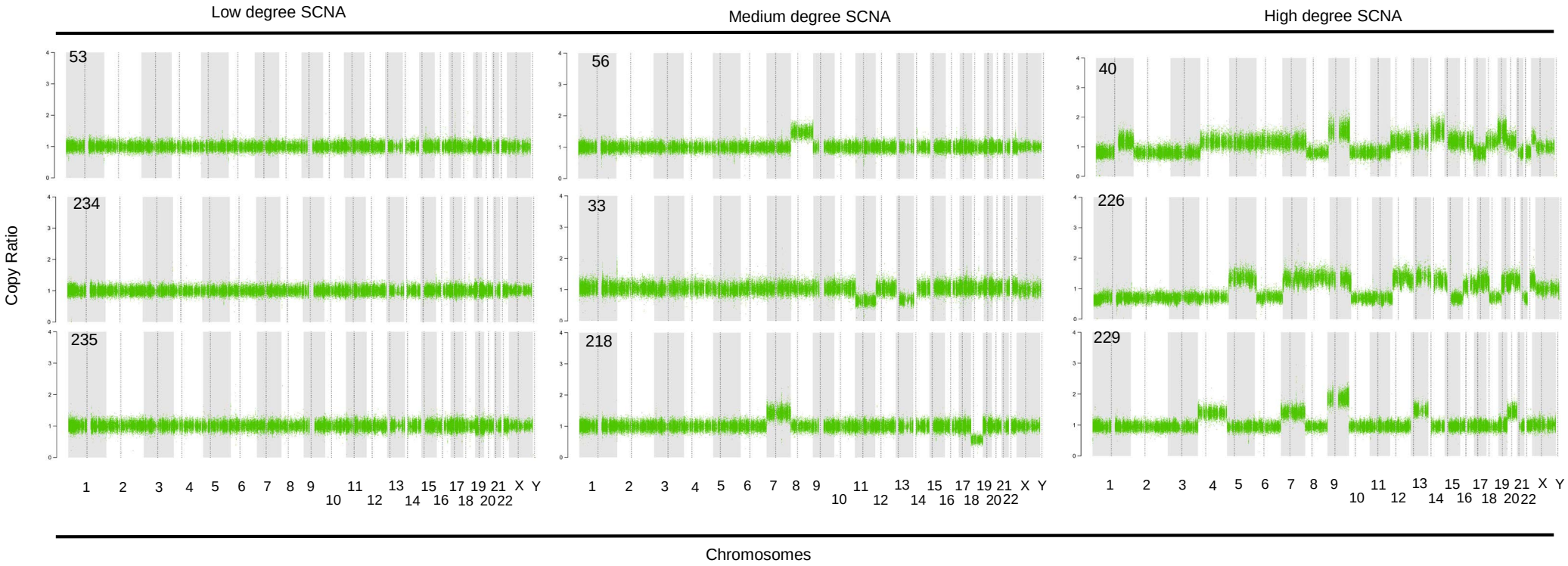

Figure S3. Visual representation of low, medium, and high degree SCNA in 9 human pituitary adenomas. Copy ratio is shown on the y-axis and chromosome number on the x-axis; adenoma number is presented in the left upper corner of each graph.

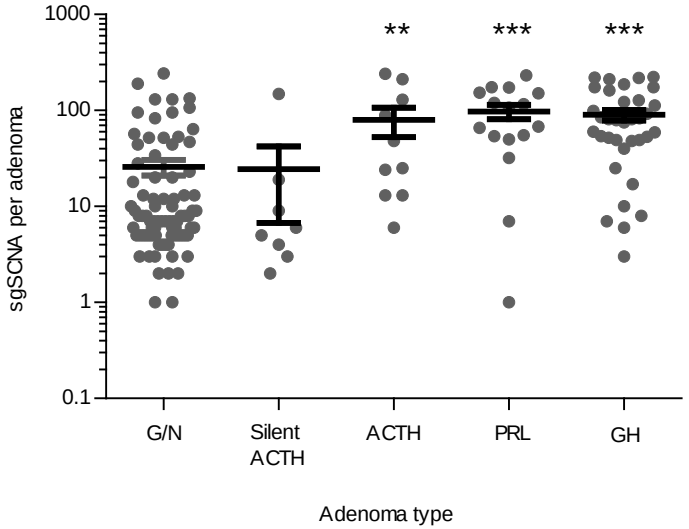

Figure S4. Number of sgSCNA per adenoma for each adenoma subtype in the entire cohort (n=159). G/N, non-secreting gonadotroph/null cell adenomas, Silent ACTH, silent corticotroph adenomas; ACTH, secreting corticotroph adenomas; PRL, lactotroph adenomas; GH, somatotroph adenomas. Results presented as number of sgSCNA per adenoma, 2-tailed unpaired t test with Bonferroni correction. **, p≤0.01 vs G/N, ***, p≤0.001 vs G/N.

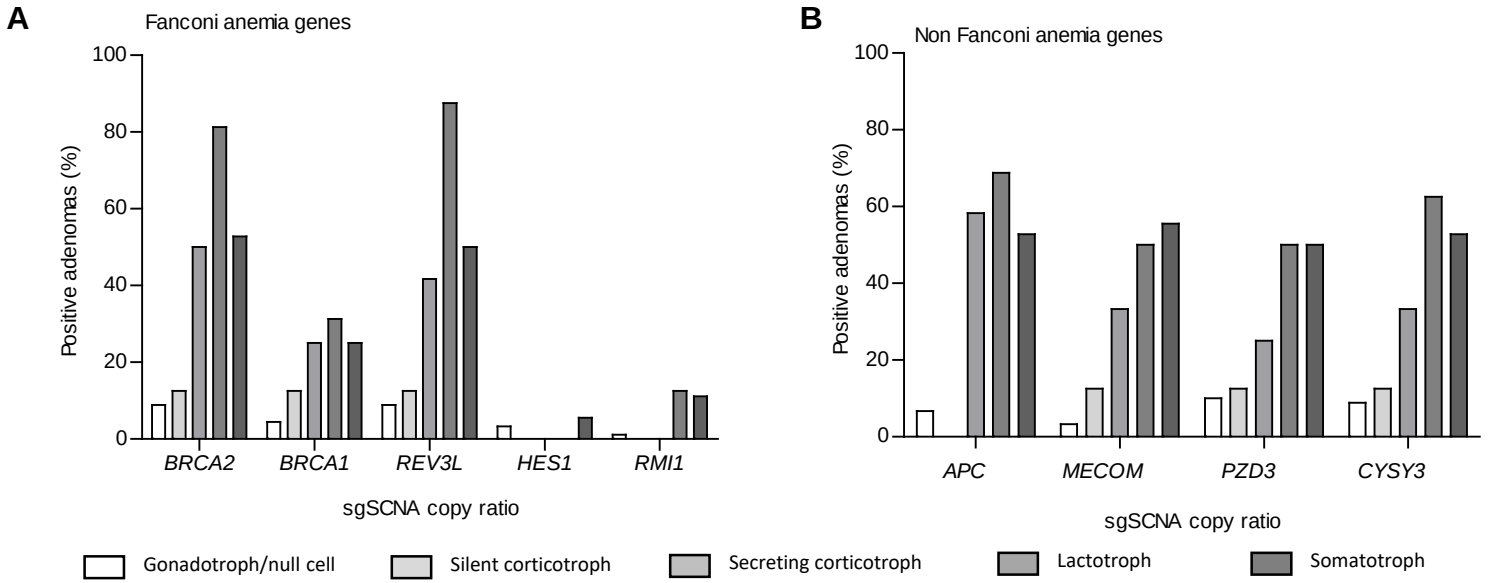

Figure S5. Frequently occurring sgSCNA genes identified in pituitary adenomas by KEGG pathway analysis. (A-B) Percent of adenomas expressing sgSCNA by adenoma subtype identified in (A) Fanconi anemia pathway (*BRCA2, BRCA1, REV3L, HES1,* and *RMI1)* and (B) pathways other than Fanconi anemia, specifically *APC* (basal cell carcinoma pathway, hsa05217), *MECOM* and *PZD3* (pathways in cancer, hsa05200), and *CYSY3* (glycosaminoglycan biosynthesis-chondroitin sulfate/dermatan sulfate pathway, hsa00532). (C-D) Correlations between adenoma SCNA copy ratio and (C) Fanconi anemia pathway sgSCNA copy ratio (Pearson *r* -0.24, p=0.006) and (D) non-Fanconi anemia pathway sgSCNA score (Pearson *r* -0.05, p=0.51). (E) sgSCNA associated genes in the cAMP pathway identified by KEGG by adenoma type. n, number sgSCNA per adenoma type, One way ANOVA with Bonferroni correction p=0.0008 for somatotroph adenomas vs other adenoma types.

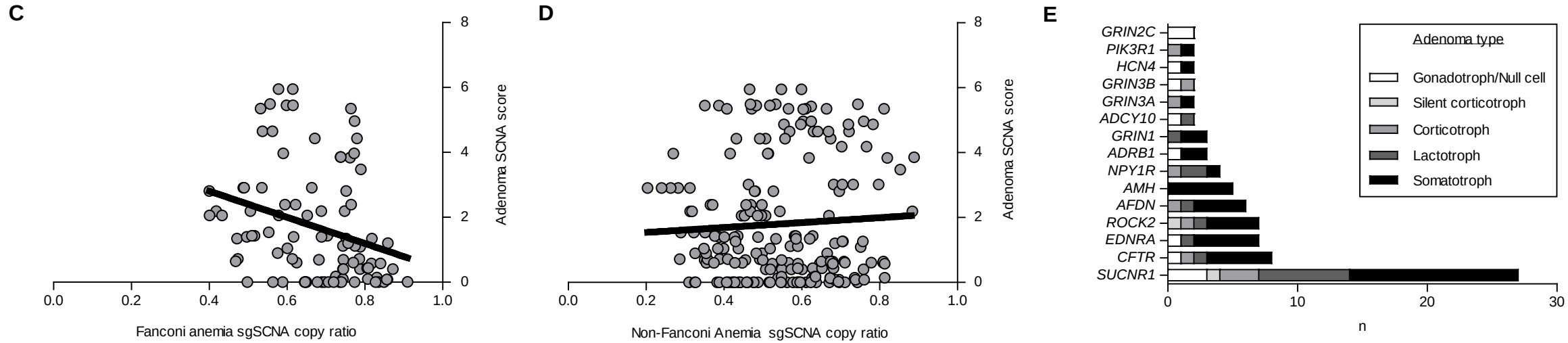

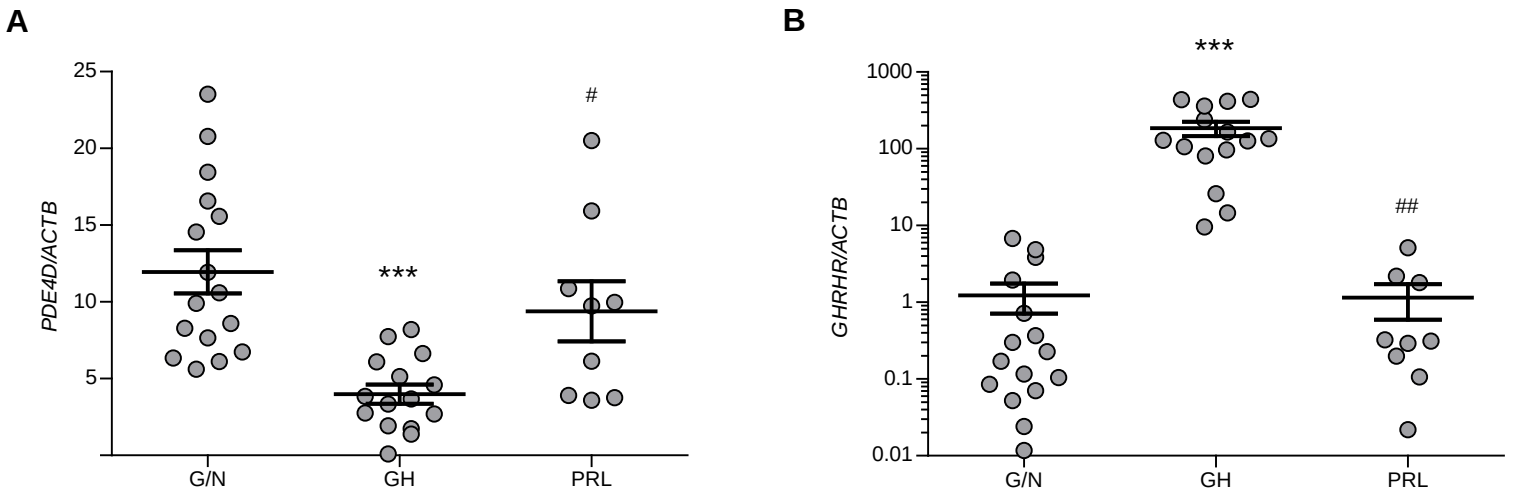

Figure S6. (A) Human *PDE4D* and (B) *GHRHR* mRNA expression in gonadotroph/null cell (G/N), somatotroph (GH), and lactotroph (PRL) pituitary adenomas normalized to β actin mRNA levels (*ACTB*). Results presented as mean ± SEM, 2-tailed unpaired t test with Bonferroni correction. *** p≤0.001 vs G/N; # p≤0.05 vs GH; ##, p≤0.01 vs GH.

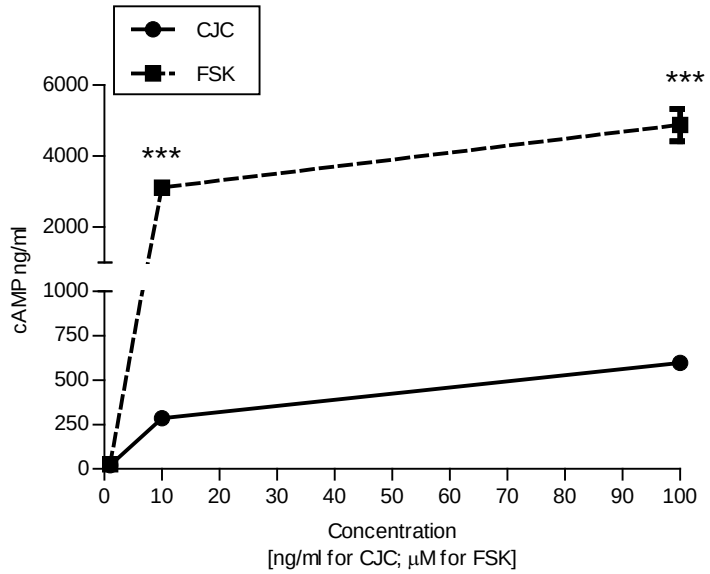

Figure S7. Dose-dependent cAMP response of normal primary pituitary cultures to 30 minutes treatment with either forskolin (FSK, µM) or CJC-1295 (CJC, ng/mL). Two-way ANOVA with Bonferroni correction. ***, p≤0.001 FSK vs CJC.

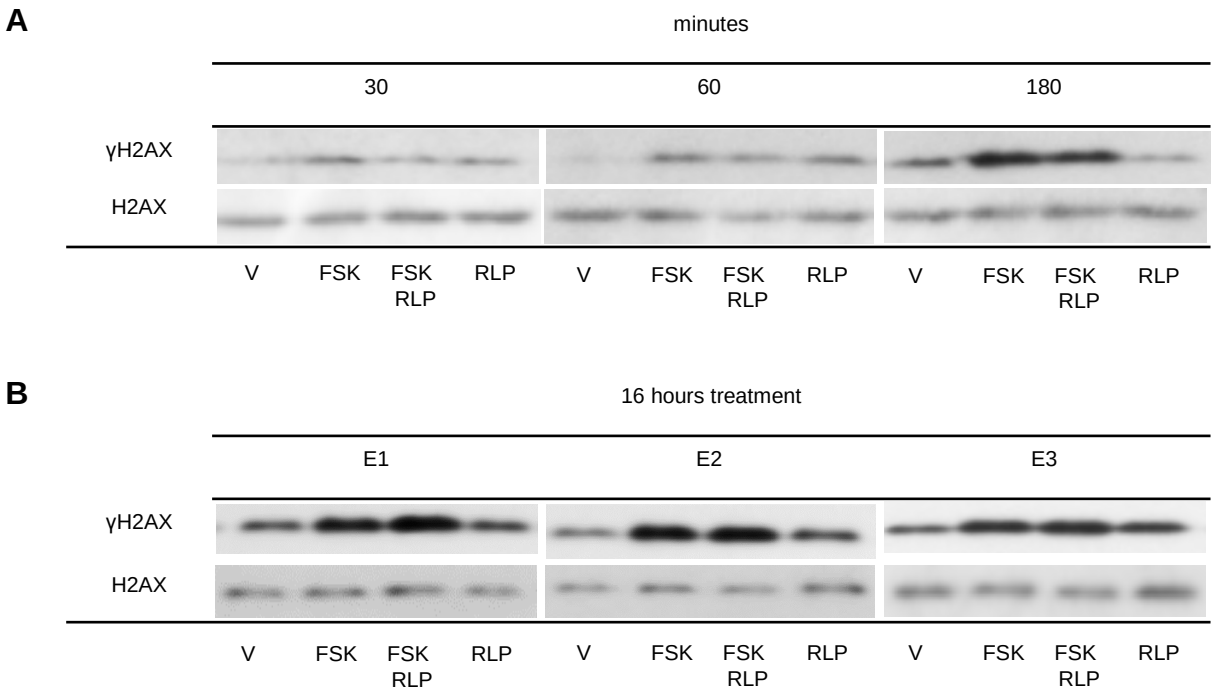

Figure S8. Normal mouse primary pituitary cultures treated with forskolin (FSK) and rolipram (RLP). (A) Western blot depicting γH2AX expression at 30, 60, and 180 minutes after treatment with vehicle (V), 10 µM FSK, co-treatment of 10 µM FSK and 1 µM RLP, or 1 µM RLP alone. Total H2AX served as normalizing control. (B) γH2AX expression after 16 hours treatment in 3 different experiments, E1, E2, and E3. Total H2AX served as normalizing control.

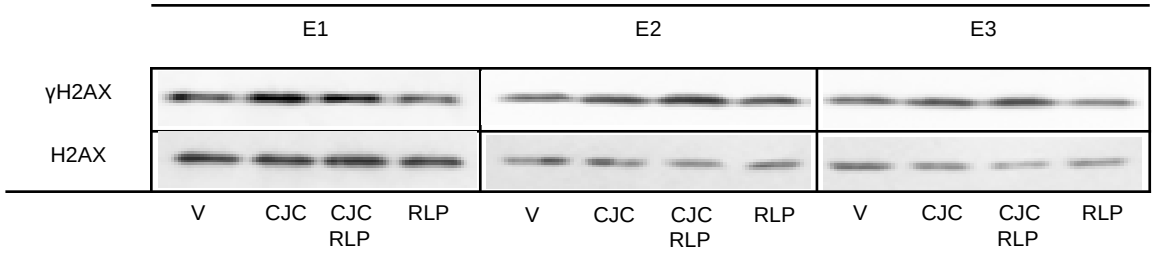

Figure S9. Normal mouse primary pituitary cultures treated with CJC-1295 (CJC) and rolipram (RLP). γH2AX expression after 16 hours treatment with vehicle (V), 10 ng/mL CJC-1295 (CJC), co-treatment with 10 ng/mL CJC-1295 and 1 µM rolipram (RLP), or with 1 µM rolipram alone in 3 different experiments, E1, E2, and E3. Total H2AX served as normalizing control.

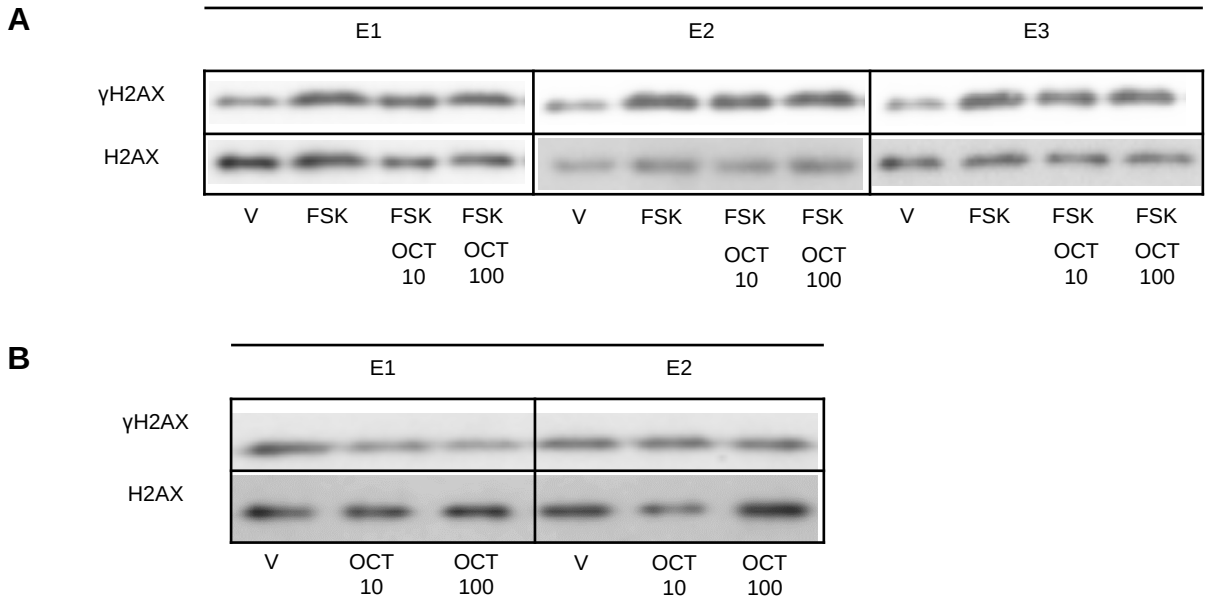

Figure S10. Normal mouse primary pituitary cultures treated with forskolin (FSK) and octreotide (OCT). (A) γH2AX expression after 16 hours of treatment with vehicle (V), 10 µM FSK, co-treatment with 10 µM FSK and 10 nM OCT (OCT 10), or co-treatment with 10 µM FSK and 100 nM OCT (OCT 100) in 3 different experiments, E1, E2, and E3. Total H2AX served as normalizing control. (B) Mouse primary pituitary cultures treated with OCT 10 and OCT 100. γH2AX expression after 16 hours treatment with vehicle (V), OCT 10, and OCT 100 in 2 different experiments, E1 and E2. Total H2AX served as normalizing control.

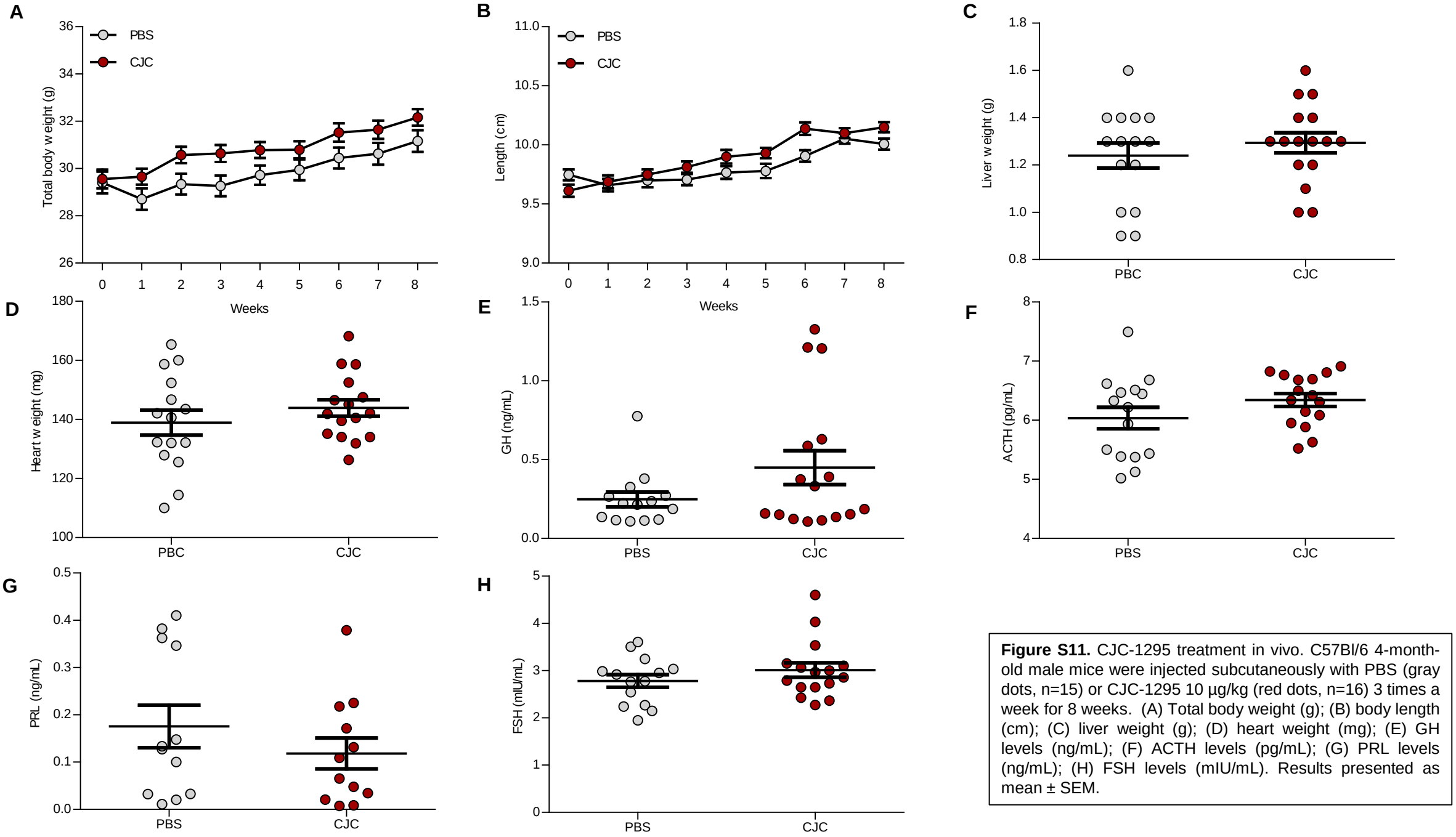

Figure S11. CJC-1295 treatment in vivo. C57Bl/6 4-month-old male mice were injected subcutaneously with PBS (gray dots, n=15) or CJC-1295 10 µg/kg (red dots, n=16) 3 times a week for 8 weeks. (A) Total body weight (g); (B) body length (cm); (C) liver weight (g); (D) heart weight (mg); (E) GH levels (ng/mL); (F) ACTH levels (pg/mL); (G) PRL levels (ng/mL); (H) FSH levels (mIU/mL). Results presented as mean ± SEM.

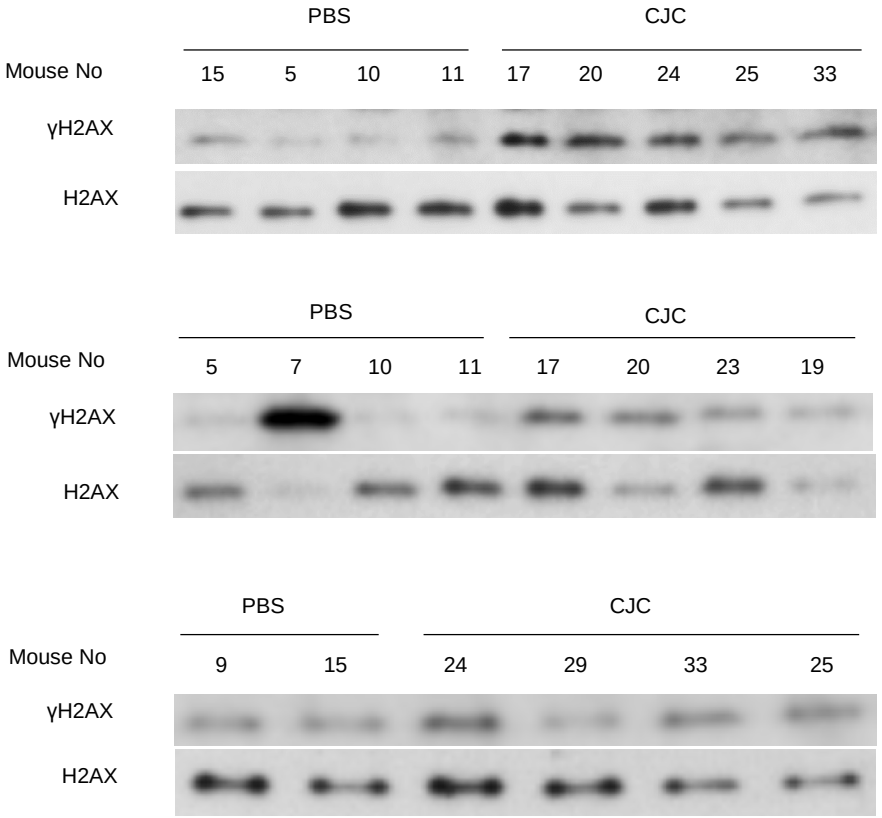

Figure S12. Western blot depicting γH2AX change normalized to total H2AX of PBS (n=6) vs CJC-1295 (CJC, n=8) mice in vivo. Numbers represent mouse identification number. One mouse was excluded from the PBS group due to very low protein retrieval and the lack of a visible H2AX on Western blot. Mouse No 7 in the PBS group was excluded as an outlier, as described in Results.